Development 136, 147-160 (2009) doi:10.1242/dev.030064

Cis-regulatory mechanisms of left/right asymmetric neuron-subtype specification in *C. elegans*

John F. Etchberger, Eileen B. Flowers, Richard J. Poole, Enkelejda Bashllari and Oliver Hobert*

Anatomically and functionally defined neuron types are sometimes further classified into individual subtypes based on unique functional or molecular properties. To better understand how developmental programs controlling neuron type specification are mechanistically linked to programs controlling neuronal subtype specification, we have analyzed a neuronal subtype specification program that occurs across the left/right axis in the nervous system of the nematode *C. elegans*. A terminal selector transcription factor, CHE-1, is required for the specification of the ASE neuron class, and a gene regulatory feedback loop of transcription factors and miRNAs is required to diversify the two ASE neurons into an asymmetric left and right subtype (ASEL and ASER). However, the link between the CHE-1-dependent ASE neuron class specification and the ensuing left-right subtype specification program is poorly understood. We show here that CHE-1 has genetically separable functions in controlling bilaterally symmetric ASE neuron class specification and the ensuing left-right subtype specification program. Both neuron class specification and asymmetric subclass specification depend on CHE-1-binding sites ('ASE motifs') in symmetrically and asymmetrically expressed target genes, but in the case of asymmetrically expressed target genes, the activity of the ASE motif is modulated through a diverse set of additional cis-regulatory elements. Depending on the target gene, these cis-regulatory elements either promote or inhibit the activity of CHE-1. The activity of these L/R asymmetric cis-regulatory elements is indirectly controlled by *che-1* itself, revealing a feed-forward loop configuration in which *che-1* restricts its own activity. Relative binding affinity of CHE-1 to ASE motifs also depends on whether a gene is expressed bilaterally or in a left/right asymmetric manner. Our analysis provides insights into the molecular mechanisms of neuronal subtype specification, demonstrating that the activity of a neuron type-specific selector gene is modulated by a variety of distinct means to diversify individual neuron classes into specific subclasses. It also suggests that feed-forward loop motifs may be a prominent feature of neuronal diversification events.

KEY WORDS: *C. elegans*, Neuronal development, Left/right asymmetry, Transcriptional regulation

INTRODUCTION

The classification of individual neuron types has a long history dating back to the work of Ramon y Cajal (Ramon y Cajal, 1911). Initially characterized by morphological criteria, more modern functional, physiological and molecular approaches have revealed an astounding diversity of cell types in the nervous system, more so than in any other organ (Masland, 2004; Nelson et al., 2006). In order to understand the development of an organ composed of such vastly diverse cell types, it is useful to study the development of the simple units that make up the organ. One approach to breaking down the nervous system into simple units is the hierarchical clustering of neurons into groups of neurons that share common features such as morphology or function ('neuron classes' or 'neuron types') and further clustering these groups into subtypes or subclasses. These subtypes share fundamental common functions or morphologies, but they differ in a restricted subset of features that define individual subtypes.

How are the regulatory mechanisms responsible for neuron type and neuron subtype specification integrated? Specifically, are the regulatory factors that control neuron type specification completely separate from those that control ensuing subtype specification or are they mechanistically linked? We address this here by exploring the specification of the bilaterally symmetric ASE neuron class in the nematode *C. elegans*. This neuron class is composed of two neurons, each defining its own subtype: the left ASE neuron (ASEL) and the right ASE neuron (ASER). Both neuron subtypes are morphologically and synaptically indistinguishable and share a large battery of co-expressed genes, but display differential asymmetric expression of a class of putative chemoreceptor genes (reviewed by Hobert et al., 2002).

ASE neuron class specification is controlled by the terminal selector gene *che-1* (Chang et al., 2003; Etchberger et al., 2007; Uchida et al., 2003). *che-1* encodes a zinc-finger transcription factor that directly controls the expression of its target genes by binding to its cognate binding sequence: the ASE motif. It is the expression of these target genes, including ion channels, neurotransmitter receptors and neuropeptide-encoding genes, that characterizes the terminally differentiated bilateral ASE neurons. While adopting their bilaterally symmetric terminal fate, the ASE neurons execute a further subtype diversification program in which the left and right ASE neurons diversify by differentially expressing distinct members of a family of putative chemoreceptors, encoded by the *gcy* genes (Fig. 1A) (Ortiz et al., 2006; Yu et al., 1997). This diversification program involves a gene regulatory loop, composed of transcription factors and miRNAs (Fig. 1A) (Johnston et al., 2005), and results in the asymmetric expression of the *gcy* genes. The expression of components of this regulatory loop, as well as the *gcy* genes themselves, is lost in *che-1* mutants and each of these genes contains ASE motifs in their promoters that are required for their expression in ASE (Etchberger et al., 2007). Therefore, CHE-1 not only determines terminal differentiation features of ASE, but also directly induces downstream regulatory events required for subtype specification.

The necessity of CHE-1 for the specification of both neuronal subtypes, ASEL and ASER, poses the question of specificity. How does CHE-1 induce solely ASEL-specific genes in ASEL and

Howard Hughes Medical Institute, Department of Biochemistry and Molecular Biophysics, Columbia University Medical Center, 701 West 168th Street, New York, NY 10032, USA.

*Author for correspondence (e-mail: or38@columbia.edu)

Accepted 22 October 2008

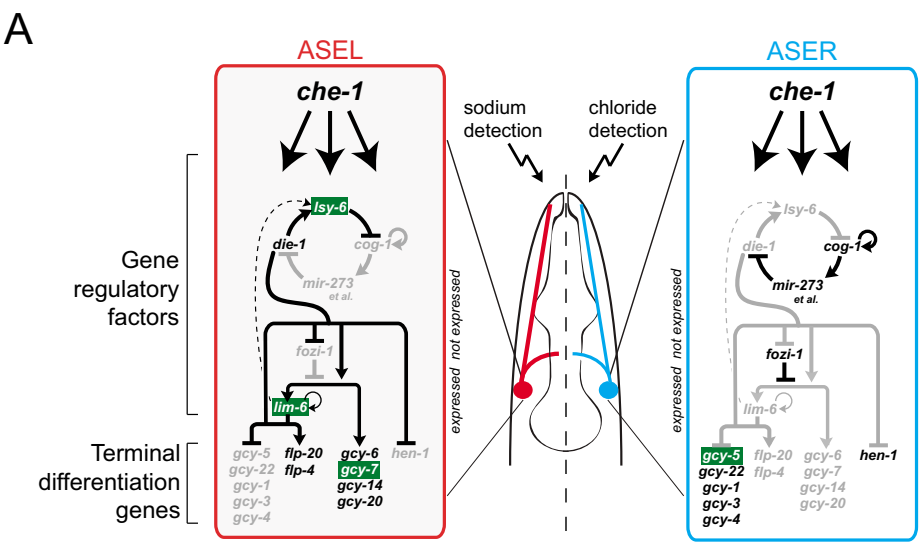

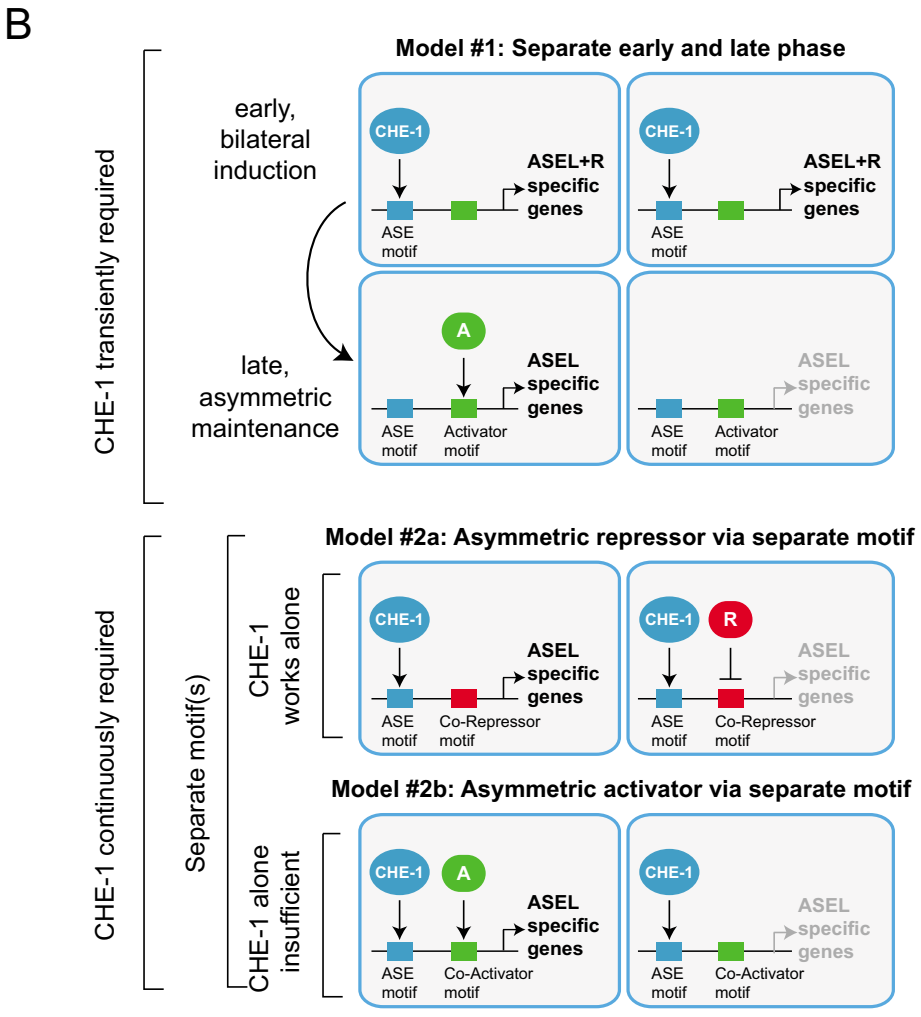

Fig. 1. Models for ASE neuron development and the establishment of left/right asymmetric gene expression profiles. (**A**) Regulatory network for ASE neuron specification. Green boxes indicate genes whose asymmetric regulation is addressed in this paper. (**B**) Three models are depicted that may explain the regulatory logic of L/R asymmetric gene expression programs in the ASE neurons. For simplicity, examples are limited to the regulation of ASEL-specific genes.

ASER-specific genes in ASER, even though CHE-1 is expressed in both ASEL and ASER, and is able to induce bilaterally expressed genes in both neurons? Genetic evidence has shown that differential expression of genes in the regulatory loop shown in Fig. 1A is required for ASE to adopt either ASEL or ASER fate, but exactly how this mechanism functions at the level of cis-regulatory motifs is unknown. We envision several distinct models that are addressed here in this paper and are schematically presented in Fig. 1B. Model 1 is based on the observation that initially after the birth of ASEL and ASER, the two ASE subtypes appear to share the expression of terminal differentiation markers that eventually become restricted to ASEL or ASER during late embryogenesis and early larval

development (Johnston et al., 2005). Model 1 posits that CHE-1 is required only for the induction of the bilateral precursor state, inducing the expression of both terminal markers (such as *gcy-7*, which is initially expressed in both ASEL and ASER) and regulatory factors that directly control ASEL or ASER-specific genes. These regulatory factors may then be sufficient to induce the L/R diversification, thereby making CHE-1 activity superfluous after this initial specification event (Fig. 1B). In Model 2, CHE-1 is required throughout the lives of the ASE neurons and actively participates in controlling the L/R asymmetry of the gene expression profiles in these cells. As CHE-1 acts in a target gene-specific manner in both ASEL and ASER, the L/R specificity cannot be brought about simply by directly modulating intrinsic CHE-1 activity (e.g. by post-transcriptional mechanisms such as protein modifications or stability). Rather, L/R specificity would need to be brought about by the repression of CHE-1 activity in a target gene-dependent manner through what we term here 'co-repressor' molecules (Fig. 1B, Model 2a). Alternatively, CHE-1 may not be sufficient to activate L/R-restricted target genes and may require what we term here 'co-activator' molecules (Fig. 1B, Model 2b).

We test these models here in a variety of ways, including temporally controlled gene knock-down, dissection of the cis-regulatory architecture of L/R asymmetrically expressed genes and various genetic manipulations. We find that L/R asymmetric gene expression programs are controlled by complex and diverse cis-regulatory control mechanisms and we show that the affinity of CHE-1 to its binding site plays a role in controlling L/R asymmetric gene expression programs.

MATERIALS AND METHODS

DNA constructs and transgenes

All *gfp* reporter constructs are based on the pPD95.75 vector and were generated either by subcloning or PCR fusion (Hobert, 2002). As indicated in the figure legends, constructs were injected either as circular subcloned DNA or as a linear PCR fragment, generated either by PCR fusion or PCR amplification of a cloned product. DNA constructs were injected into an *otIs151* background, which expresses a *ceh-36::DsRed2* transgene to facilitate the identification of expression of *gfp*-based reporter genes in ASEL/R. The gut-specific *elt-2::gfp* reporter (a gift from J. McGhee) was used as an injection marker. Mutagenesis reactions were performed using the QuickChange II XL Site Directed Mutagenesis Kit (Stratagene). A list of DNA sequences can be provided on request.

RNAi assays

RNAi by feeding was performed (see Ahringer, 2005) in the *nre-1 lin15b* sensitized background (Schmitz et al., 2007). For scoring of F1s, 10-15 staged L3/L4 hermaphrodites were placed onto plates seeded with dsRNA-expressing clones and incubated for 5 days at 22°C before scoring the F1 progeny as adults on a Zeiss axioplan microscope. In the case of P0 scoring, 100-150 staged L1s were placed on the plates and incubated for 3-4 days before scoring as adults.

Electrophoretic mobility shift assay (EMSA)

CHE-1 and CEH-36 proteins were expressed and purified, and binding reactions were performed (see Etchberger et al., 2007). For quantitative cold competition assays, different types of cold competitor (ASE motifs from genes tested) were added at specific ratios relative to the labeled *ceh-36* probe to the protein/*ceh-36* probe mixture after 10 minutes of the initial binding reaction and allowed to incubate with the protein/probe complex for an additional 10 minutes before loading on the gel. After detection of bound probe using the Molecular Dynamics PhosphorImager and quantification with ImageJ, the fraction of bound labeled *ceh-36* probe compared with bound uncompeted probe was plotted against the molar ratio of unlabeled to labeled probe (Glass et al., 1988). The affinities of each probe relative to the *ceh-36* probe were calculated by comparing the slopes of a plot of [(1–Y)/Y] versus amount of competitor, where Y is the fraction of bound labeled probe at a given ratio of unlabeled to labeled probe (Glass et al., 1988).

RESULTS

che-1 is required to initiate and maintain neuronal fate in ASE

che-1 null mutant animals do not initiate ASE differentiation, as evidenced by a complete lack of expression of ASE differentiation markers at all stages of embryonic development (Chang et al., 2003) (data not shown). To assess whether the function of *che-1* function is restricted to the initiation of ASE differentiation or extends to the maintenance of the differentiated state (Fig. 1B, Model 1 versus Model 2), we reduced *che-1* activity in a temporally restricted manner by performing RNAi on transgenic animals expressing either an ASEL-specific marker (*lim-6::gfp*) or an ASER-specific marker (*gcy-5::gfp*). The ASE neurons undergo their final division at ~380 minutes post-fertilization (Sulston et al., 1983). *che-1* expression can be observed as early as one cell division before the birth of ASEL and ASER, and persists through adulthood (B. Tursun and O.H., unpublished). We delivered *che-1* dsRNA by feeding animals at the larval L1 stage (i.e. long after ASE has been generated in mid-embryogenesis). If *che-1* activity was required solely for the initiation of gene expression in ASEL/R, then only the F1 progeny of RNAi-treated animals and not the P0 animals should show a loss or reduction of *gfp* expression. If *che-1* activity was continuously required during the lifetime of the animal, the removal of *che-1* would result in a loss or reduction of *gfp* expression in the acutely RNAi-treated P0 animals. After treatment of staged L1 animals with *che-1* RNAi, we observed a significant reduction of both ASEL-specific and ASER-specific marker expression in both ASEL and ASER in adult P0 animals (Fig. 2A,B). These results indicate that *che-1* is required not only for the initiation but also for the maintenance of gene expression in ASEL/R.

Testing cis-regulatory models for the control of L/R asymmetric gene expression

The continuous requirement of *che-1* activity for ASEL/R gene expression means that L/R asymmetric transcription of terminal differentiation genes necessitates a mechanism that restricts the activity of bilaterally expressed CHE-1 in a target gene-dependent (i.e. promoter-dependent) manner to either ASEL or ASER. 'Promoter-dependent' means that bilaterally expressed genes respond to CHE-1 in both ASEL and ASER, whereas L/R asymmetrically expressed genes respond only to CHE-1 in either ASEL or ASER. As mentioned in the Introduction, this may involve either promoter-dependent co-activator or co-repressor mechanisms (Fig. 1B). To test these models, we analyzed the cis-regulatory architecture of four asymmetrically expressed genes that are direct targets of *che-1*, as they each contain ASE motifs required for expression in the ASE neurons (Etchberger et al., 2007; Sarin et al., 2007): two putative chemoreceptors of the guanylyl cyclase family, ASEL-expressed *gcy-7* and ASER-expressed *gcy-5* (Yu et al., 1997); the ASEL-expressed LIM-homeodomain transcription factor *lim-6* (Hobert et al., 1999); and the ASEL-expressed microRNA *lsy-6* (Johnston and Hobert, 2003). The activation model (Fig. 1B, Model 2b) predicts that the ASE motifs of each of these genes are not alone sufficient to promote expression in both ASE neurons, whereas the repression model (Fig. 1B, Model 2a) predicts that the ASE motif alone can drive expression in both ASE neurons. We find that each isolated ASE motif from the four asymmetrically expressed genes when fused to *gfp* produces reporter gene expression in both ASE neurons (Fig. 3). As this bilateral expression is lost in the context of larger regulatory elements, these regulatory elements must therefore contain information that somehow restricts CHE-1 and ASE motif

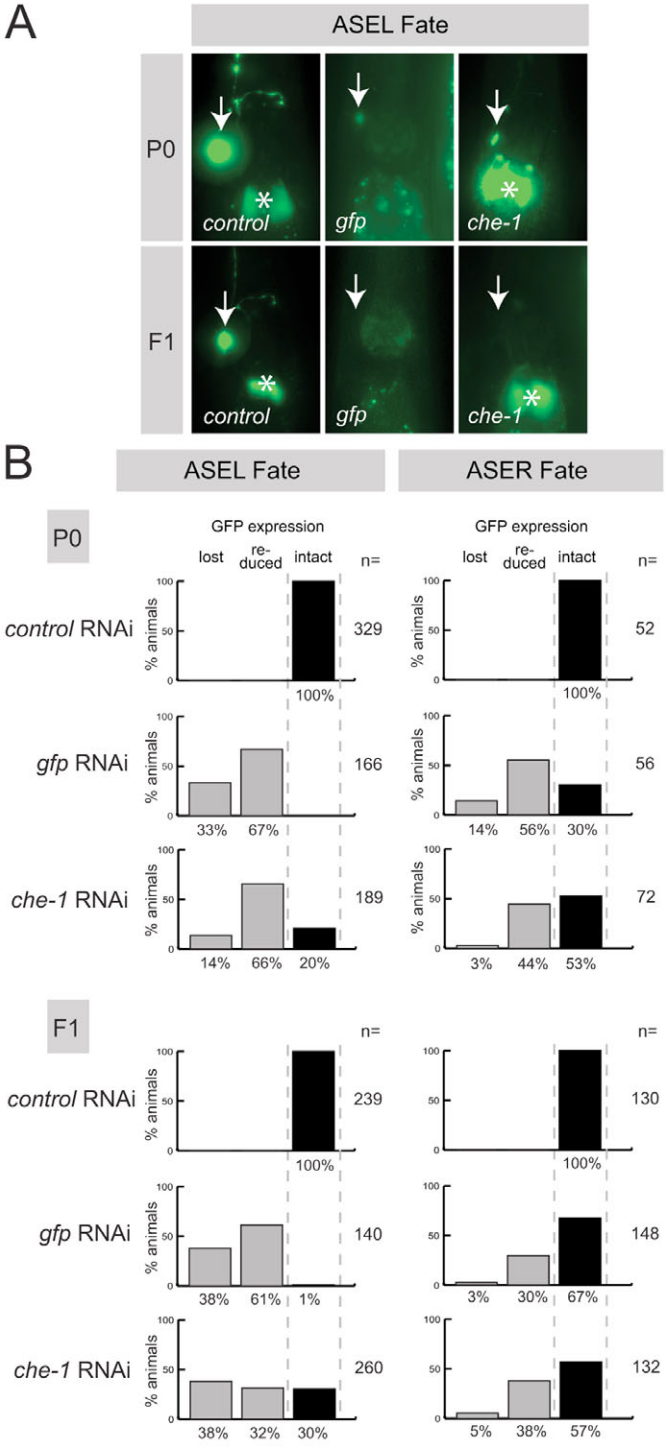

Fig. 2. Effect of postdevelopmental *che-1* RNAi on the execution of ASE terminal fate. (**A**) Representative examples for RNAi effects on the ASEL fate marker *lim-6::gfp*, expressed in ASEL (arrows) and on the excretory gland cells (asterisks), which serve as internal controls, as they are not affected by control or *che-1* RNAi, but are affected by *gfp* RNAi. Control RNAi refers to RNAi with empty vector L4440. Note the differences in *gfp* intensities for *che-1* RNAi; as quantified in B, either a reduction of *gfp* levels (as shown in A) or a complete loss was observed. (**B**) A quantification of effects of *che-1* RNAi on ASEL (*lim-6::gfp*) and ASER marker (*gcy-5::gfp*) results are shown.

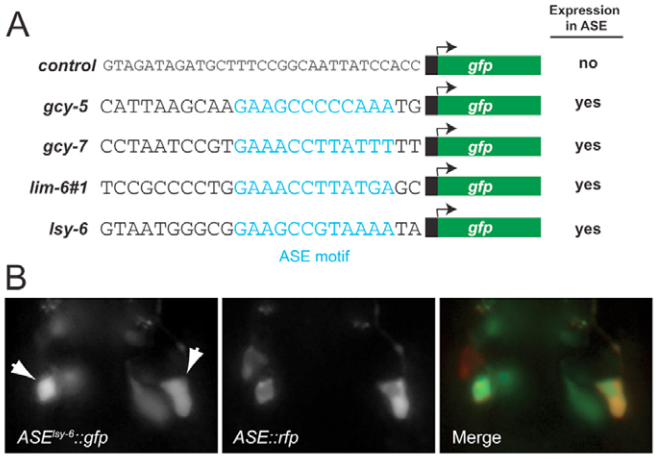

Fig. 3. The ASE motif from ASEL- and ASER-specific genes directs bilateral expression in the ASE neurons. (**A**) 24 bp encompassing the ASE motifs from ASEL-specific (*lsy-6*, *gcy-7* and *lim-6*) and ASER-specific (*gcy-5*) genes are fused via PCR into the multiple cloning site of the *gfp* expression vector pPD95.75, which contains an uncharacterized basal promoter before the *gfp* start codon. To exclude the possibility that the basal promoter has any ASE-regulatory information, a 21 bp sequence with no obvious match to the ASE motif was also tested as control and found to not be expressed in ASE; empty vector also produces no expression (data not shown). ASE expression of the *gcy-5* ASE-motif construct has been described previously with no mention of the symmetry of its expression (Etchberger et al., 2007). (**B**) Representative images of the *lsy-6* ASE motif driving expression of *gfp* in ASEL/R. Multiple lines show similar expression for all constructs listed in A. In all cases, expression in the ASE neurons was assessed with a *ceh-36*^{prom}*::DsRed2* (*otIs151*) transgene contained in the background. Arrows indicate ASEL and ASER.

activity. To dissect the nature of the additional regulatory information, we undertook a systematic deletion analysis of the L/R asymmetrically expressed regulatory regions of these genes (Fig. 4).

Case 1: *gcy-7*

We conducted a scanning mutagenesis of the cis-regulatory region that is required and sufficient for the ASEL-specific expression of *gcy-7* (gcy-7^{prom2}, 188 bp) (Etchberger et al., 2007). We first created seven non-overlapping deletion windows of 22-32 bp in length (Fig. 4A). Previous results have shown that the *che-1*-responsive ASE motif of the *gcy-7* promoter lies at the junction of deletion windows 3 and 4, the only deletions that resulted in loss of expression in ASEL (Etchberger et al., 2007). Of the seven deletion windows, three constructs (del2, del5 and del7) show a partially penetrant de-repression of *gfp* expression in ASER (Fig. 4A; see Figs S1 and S2 in the supplementary material). A triple deletion (del2,5,7) does not further increase the penetrance of de-repression, even though the levels of de-repressed *gfp* appear to be somewhat increased (Fig. 4A; see Fig. S2 in the supplementary material). These findings support the 'co-repressor model' in Fig. 1B.

To refine our mapping of the repressive regulatory architecture, we generated smaller deletions within the identified repressive sequences. For all three regions, our analysis revealed discrete repressive sequences 6-8 bp in length that recapitulated the derepression effects of the larger deletions (del2b; del4b; del7a) (Fig. 4A; see Fig. S2 in the supplementary material). We also

deleted small phylogenetically conserved motifs within the ASE motif-containing region del3 (del3a) (see Fig. S3 in the supplementary material) and deletion window 6 (del6a) (see Fig. S3 in the supplementary material). As a result of both deletions, we observed partial derepression of *gfp* in ASER (Fig. 4A; see Fig. S2 in the supplementary material). None of the four small motifs show notable similarities to one another, but each is phylogenetically conserved in the *gcy-7* promoter of three other nematode species (see Fig. S3 in the supplementary material). One of the four motifs, del4b, matches a predicted NK-2 homeodomain binding site (TAAGTT) (Noyes et al., 2008). Other ASEL-specific *gcy* genes have some, but not all, of these motifs. We deleted two of these motifs (TTCGGGAG and GGAAAAAA) in *gcy-14* and *gcy-20*, but these deletions did not affect ASEL-specific expression of these genes (data not shown).

We noted a predicted K50-homeodomain binding site (TAATCC) directly downstream of the ASE motif. Deletion of this motif (del4a) from the *gcy-7* minimal promoter resulted in a loss of *gfp* expression in ASEL. This is surprising as this deletion construct retains its ASE motif, which, like any other ASE motif tested, drives bilateral expression in complete isolation (Fig. 3). In the context of the *gcy-7* promoter, the CHE-1-binding ASE motif, therefore, needs to collaborate with a 'co-activator' motif (Fig. 1B, Model 2b) to activate ASEL-specific expression.

The 'co-activator' motif also confers a left/right asymmetric activity to the ASE motif as a construct that contains only the ASE motif and the neighboring co-activator motif is asymmetrically expressed, with *gfp* levels in ASEL being substantially higher than in ASER (Fig. 4A) (compare $ASE^{gcy\text{-}7\#1}$ with $ASE^{gcy\text{-}7\#2}$). In other words, such a minimal motif is derepressed in ASER owing to the loss of the repressor motifs described above, but it still retains L/R asymmetry to some degree.

Intriguingly, the loss of ASE expression observed upon loss of the co-activator motif (del4a) is completely suppressed if the del4a deletion is combined with deletions of the three repressor motifs: del2, del5 and del7. The resulting quadruple mutant construct is expressed in a bilaterally symmetric manner in both ASEL and ASER (Fig. 4A). We interpret these findings to mean that the ASE motif of *gcy-7* can, in principle, drive bilateral expression in ASEL and ASER; this activity alone is repressed through repressive cis-regulatory motifs, but the presence of the TAATCC motif can overcome this repression specifically in ASEL (Fig. 4A). In summary, *gcy-7* is regulated by a combination of the 'co-activator' and 'co-repressor' models as shown in Fig. 1B.

Case 2: *gcy-5*

We started the analysis of the cis-regulatory region of the *gcy-5* gene again with a scanning deletion analysis on the fragment of the *gcy-5* regulatory control region ($gcy\text{-}5^{prom2}$, 306 bp), which is required and sufficient to drive ASER-specific expression of a reporter gene (Etchberger et al., 2007). We deleted, in a non-overlapping manner, 24-31 bp windows (Fig. 4B). Three of the 11 deletion windows (del3, del7 and del11) each resulted in a low penetrant de-repression of *gfp* expression in ASEL, while leaving expression in ASER unaffected (Fig. 4B; see Figs S1 and S2 in the supplementary material). Double (del7,11) and triple deletions (del3,7,11) exhibited an increase in the penetrance of de-repression of *gfp* in ASEL (see Fig. S2 in the supplementary material). However, neither the double nor triple deletion constructs showed equivalent bilateral expression in ASEL/R. Bilateral expression is observed, however, if all sequences around the ASE motif are chopped away, leaving only a 24 bp minimal element (Fig. 3) (Etchberger et al., 2007). We conclude that repressive elements within region 3, 7 and 11 are, in part, responsible for repression of *gcy-5* expression in ASEL. Notably, in contrast to the *gcy-7* regulatory region, the *gcy-5* regulatory region does not appear to contain a 'co-activator' motif as no mutation other than the ASE motif deletion results in a loss of reporter gene expression.

To define individual sequence motifs within these repressive regions, we created smaller deletions within each repressive region in an attempt to recapitulate the derepression resulting from the larger individual deletions (Fig. 4B; see Fig. S2 in the supplementary material). For del3 and del7, we were able to identify short sequences (8 bp and 7 bp, respectively), the loss of which resulted in de-repression of *gfp* expression in ASEL. Neither motif shows unambiguous matches to known transcription factor-binding sites predicted by MatInspector (Cartharius et al., 2005). For del11, we were unable to identify any discrete motif, even though our smaller deletions targeted nearly the entire original deletion window (Fig. 4B; see Fig. S2 in the supplementary material).

The repressor motifs share little sequence similarity with each other and are not conserved in *C. briggsae*. The *C. briggsae gcy-5* promoter, when injected into *C. elegans*, does not drive detectable *gfp* expression in ASE neurons (data not shown). This finding is also consistent with our previous observations that, in spite of strong synteny of at least some of the individual loci, the regulation of several other *gcy* genes and also their genomic organization has significantly diverged in *C. briggsae* (Ortiz et al., 2006). Last, we also did not find the motifs conserved in other ASER-restricted *gcy* genes, such as *gcy-1* and *gcy-22*.

Case 3: *lim-6*

Previous promoter analysis has identified a 200 bp minimal cis-regulatory sequence of the *lim-6* locus that is required and sufficient to direct expression of a *gfp* reporter gene in ASEL (Etchberger et al., 2007). We generated eight non-overlapping deletions of 24-28 bp within the minimal *lim-6* promoter. Four out of the eight deletions (del4, del6, del7 and del8) resulted in the loss of *gfp* expression in ASEL (Fig. 4C) (Etchberger et al., 2007). In contrast to our analysis of *gcy-5* and *gcy-7*, none of the deletions resulted in the derepression of *gfp* in ASER.

The *lim-6* minimal promoter contains two ASE motifs, one in deletion window 6 and one in deletion window 7. The targeted deletion of each of these ASE motifs individually resulted in a loss of *gfp* expression (Etchberger et al., 2007). However, as mentioned above, two additional deletion windows, del4 and del8, also resulted in loss of *gfp* expression (Etchberger et al., 2007). The del4 and the del8 sequence share no similarity with the ASE motif consensus sequence or with one another. They are also poorly conserved in other nematode species (see Fig. S3 in the supplementary material).

To identify the positive-acting cis-regulatory motif(s) in each region, we generated sub-deletions. No sub-deletion in del8 recapitulated the effect of the complete deletion, but within del4, two adjacent deletions, del4a and del4d, resulted in a loss of *gfp* expression in ASEL (Fig. 4C). In contrast to the temporally persistent loss of expression observed from the del4 construct, both del4a and del4d displayed normal ASEL-specific expression up to early larvae stages (L1/L2), but not in later staged larvae or adults (Fig. 4C).

Taken together, the ASE motifs of *lim-6*, even though supporting bilateral expression in isolation, are prevented from doing so in a full promoter context and require additional co-activator motifs to support expression in ASEL.

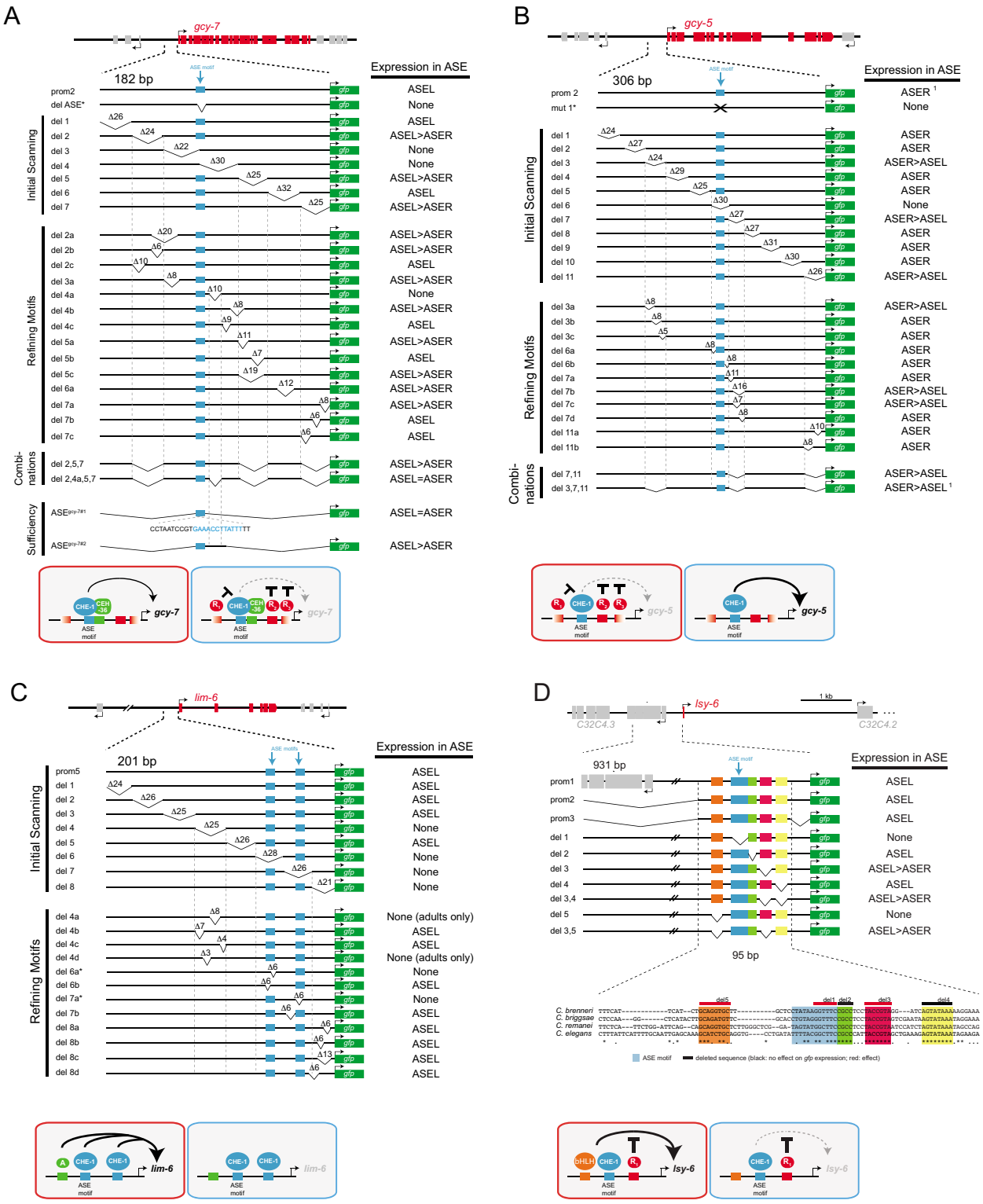

Fig. 4. See next page for legend.

Case 4: *lsy-6*

The 931 bp intergenic region between the *lsy-6* miRNA hairpin and its upstream gene contains all the regulatory information required for ASEL-specific expression and function of the ASEL-fate inducer *lsy-6* (Johnston and Hobert, 2003; Sarin et al., 2007). Successive deletions identified a 95 bp element (prom3) that is sufficient to recapitulate expression only in ASEL (Fig. 4D). As the *lsy-6* locus is highly conserved across four nematode species (Fig. 4D), we used sequence conservation as a guide for further deletion analysis. We deleted four conserved sequence patches contained within the minimal 95 bp regulatory element. Deletion of a putative E-box, a predicted bHLH protein-binding site (del5; CANNTG) resulted in a complete loss of *gfp* expression. Therefore, as in the case of *gcy-7* and *lim-6*, within its normal genomic context, the ASE motif (which

Fig. 4. Cis-regulatory analysis of L/R asymmetrically expressed genes. In all panels, *gfp* expression was scored in ASEL and ASER. Derepression of *gfp* expression in one neuron to levels that do not approach normal *gfp* levels in the contralateral neuron are indicated by 'ASEL>ASER' or 'ASEL<ASER'; similar expression levels by 'ASEL=ASER'. The incomplete nature of derepression in the contralateral neuron may relate to the multicopy structure of extrachromosomal arrays. Multiple independent transgenic lines were scored for each construct. See Fig. S1 for primary *gfp* data, Fig. S2 for quantification of data (i.e. penetrance of effects in a representative transgenic line) and Fig. S3 for nucleotide sequences (supplementary material). Deletion constructs for the *gcy-7, gcy-5* and *lim-6* promoters have been described before in the context of identifying the ASE motif (blue arrow, blue box) (Etchberger et al., 2007), but have not been reported for the effect on L/R asymmetry. (**A**) Cis-regulatory analysis of the *gcy-7* locus. All constructs are subcloned reporters except $ASE^{gcy\text{-}7\#2}$, which were generated by PCR fusion in order to minimize potential effects of vector backbone sequence. Lower panel: model of regulation for asymmetric expression of *gcy-7*, based on: (1) the partial derepression of *gfp* upon removal of del2,5,7, which argues for the presence of some other asymmetry input; (2) the requirement for del4a activator motif to drive expression in ASEL in the presence of the del2,5,7 motifs; (3) the lack of a requirement for del4a activator motif to drive expression in ASEL in the presence of the del2,5,7 motifs; and (4) the ability of the CEH-36 binding site del4 to introduce a left/right bias to the ASE motif. In ASEL, expression is induced by *che-1* and *ceh-36*. In ASER, multiple distinct repressive motifs and the absence of an activation mechanism result in the inhibition of *che-1*-mediated gene expression. Additionally, a motif in the del6 region (del6a) was deleted owing to the high level of sequence conservation and resulted in derepression of *gfp* in ASER (see Figs S2 and S3 in the supplementary material). The original scanning deletion, del6, did not result in derepression of *gfp.* (**B**) Cis-regulatory analysis of the *gcy-5* locus. The ASE motif mutated constructs ('mut1') has been described previously (Etchberger et al., 2007) and is shown for comparison only. [1]These constructs were also examined as linear PCR fragments; the wild-type promoter yields a 'ASER>ASEL' pattern and the del3,7,11 construct yields a 'ASER=ASEL' pattern. Lower panel: model of regulation for asymmetric expression of *gcy-5*, based on: (1) the observed derepression of *gfp* in ASEL from the del3,7,11 construct; and (2) the sole requirement of the ASE motif for expression in ASE. (**C**) Cis-regulatory analysis of the *lim-6* locus. All constructs were injected as subcloned circular DNA. Lower panel: model of regulation for asymmetric expression of *lim-6*, based on: (1) the complete loss of expression of *gfp* observed in ASEL from the del6 and del7 constructs; (2) the loss of maintained *gfp* expression in ASEL from the del4a/d constructs, which suggests an asymmetric activation factor is required for the maintained asymmetric expression of *lim-6*. (**D**) Cis-regulatory analysis of the *lsy-6* locus. All constructs were generated by PCR fusion as subcloned reporter constructs yielded only very weak *gfp* expression (Sarin et al., 2007). Lower panel: model of regulation for asymmetric expression of *lsy-6*, based on: (1) the loss of *gfp* expression following the deletion of the E-box (del5); and (2) the observed ectopic expression from del4.

remains intact upon deletion of the E-box) is not sufficient to drive ASE expression but requires an additional regulatory motif to be active. Moreover, we found that deletion of another conserved motif, del3, resulted in a completely penetrant de-repression of *gfp* expression in ASER (Fig. 4D, see Fig. S2 in the supplementary material) (*gfp* de-repression is only partially expressive and cannot be further enhanced in a del3; del4 double deletion). No obvious transcription factor-binding sites match this sequence, as assessed by MatInspector (Cartharius et al., 2005).

Similar to the *gcy-7* case, the loss of *gfp* expression observed upon deletion of the E-box containing co-activator motif is suppressed if the repressor motif del3 is also mutated. The E-box therefore functions to counteract the co-repressor motif del3. If the co-repressor motif is absent, the co-activator motif becomes superfluous and the ASE motif can function in isolation. Notably, though, the ASE-motif-dependent expression in the del3/del5 double mutant is still biased to ASEL, suggesting additional mechanisms to confer L/R asymmetry.

Taken together, the restriction of ASE motif activity in the *lsy-6* promoter appears most similar to that of *gcy-7*: each promoter contains repressive elements and in each case additional co-activator motifs are required for ASE motif expression. However, the identified cis-regulatory elements share no similarity to one another.

In conclusion, the four cases analyzed here demonstrate that the regulation of asymmetric gene expression in ASEL/R requires a remarkably distinct spectrum of cis-regulatory mechanisms that differ in a gene-specific manner. In each case, promoters contain an ASE motif that in complete isolation drives bilaterally symmetric expression in ASEL and ASER. In the context of its normal promoter, ASE motifs do not display this sufficiency. The activity of the ASE motif either becomes restricted by repressive cis-regulatory elements; or it becomes dependent on the presence of additional activating cis-regulatory motifs; or it becomes restricted by a combination of both co-activators and co-repressors. None of the isolated additional cis-regulatory elements displays any similarity to one another.

The CEH-36 Otx homeodomain protein binds to a L/R asymmetry-controlling motif

How are the co-activator and co-repressor motifs identified above regulated? Previous genetic analysis has revealed a number of transcription factors involved in determining L/R asymmetry (Fig. 1A). However, little to no information about possible binding sites of these transcription factors exists, with the exception of the K50-homeodomain protein CEH-36, a *C. elegans* OTX homolog and the only K50-homeodomain protein known to be expressed in ASE (Lanjuin et al., 2003). K50-homeodomain proteins bind to a TAATCC core consensus sequence (Treisman et al., 1989) and such a sequence is required for the L/R asymmetric activation of *gcy-7* in ASEL (Fig. 4A) (del4a) (see Fig. S3 in the supplementary material). Notably, the mutant phenotype of *ceh-36* is consistent with *ceh-36* activating *gcy-7* expression, as *gcy-7* expression is lost in *ceh-36* mutants (Chang et al., 2003). We find that bacterially produced CEH-36, but not two other tested homeodomain proteins, can indeed bind to the TAATCC motif in vitro (see Fig. S4 in the supplementary material). CEH-36 binding occurs in parallel and independent of the binding of CHE-1 to the neighboring ASE motif (see Fig. S4 in the supplementary material). Of the other ASEL-specific *gcy* genes (*gcy-6*,*-14*,*-20*), or any other ASEL-specific regulatory factor (*lim-6*, *lsy-6*), only the regulatory region of *gcy-14* contains a TAATCC motif in its functionally relevant regulatory region (*lsy-6* also contains such a motif but it is not required for its correct expression; data not shown), thereby corroborating the overall theme that the mechanisms of L/R asymmetric regulatory control are diverse.

The contribution of ASE motif affinity to bilateral versus asymmetric ASE motif activity

Apart from cis-regulatory motifs that collaborate with the ASE motif, we asked whether intrinsic features of an ASE motif may also bear relevance to its bilateral versus L/R asymmetric activation. Specifically, we wondered whether the ASE motifs of asymmetrically expressed genes have a weaker affinity for CHE-

1 compared with the affinity of bilaterally expressed ASE motifs, which would allow co-activating and co-repressing cis-regulatory mechanisms to modulate the activity of the ASE motifs of asymmetrically expressed genes. This hypothesis was prompted by the creation of a metric, the 'ASE motif score', which measures the quality of a match of a given ASE motif to the ASE motif consensus sequence (Etchberger et al., 2007). According to this metric, the asymmetrically expressed *gcy-5* gene has a lower motif score than the bilaterally expressed *ceh-36* gene (0.63 versus 0.72 in a scale from 0.56 to 0.73) (Etchberger et al., 2007). To put the relevance of this metric to an experimental test, we performed electrophoretic mobility shift assays and found that bacterially produced CHE-1 indeed binds the ASE motif from *ceh-36* with higher affinity than the ASE motif from the *gcy-5* locus (Fig. 5A,D). The basis for the difference in motif score and binding affinity appears to be a differential contact of the respective ASE motifs by CHE-1. Mutating individual zinc fingers and testing mutated proteins in gel shift assays demonstrates that CHE-1 contacts the *ceh-36* ASE motif with three out of its four zinc fingers, whereas it contacts the *gcy-5* ASE motif only with two out of four zinc fingers (Fig. 5A).

The low-affinity binding site in *gcy-5* may be required to enable the negative regulatory elements ('co-repressor motifs') described above to counteract bilateral ASE motif activation. This hypothesis makes the prediction that if the low affinity ASE motif in the *gcy-5* locus were switched with a high affinity ASE motif from the *ceh-36* locus, the *gcy-5* promoter may become active in both ASEL and ASER. We indeed find that a mere substitution of 4 bp, which transforms the *gcy-5* ASE motif into that of the *ceh-36* ASE motif, causes de-repression in ASEL (Fig. 5B). To test whether this logic also applies to an ASEL-specific gene, we analyzed the *gcy-14* promoter, which also contains an ASE motif with a motif score lower than that of *ceh-36* (0.69 versus 0.72). We experimentally confirmed the lower affinity of the *gcy-14* ASE motif compared with that of the *ceh-36* ASE motif using competitive gel shift assays (Fig. 5D). As is the case for *gcy-5*, swapping the *gcy-14* ASE motif with that of *ceh-36* within the context of the *gcy-14* promoter also results in bilateral expression of the reporter (Fig. 5B).

Although the logic of asymmetrically expressed genes harboring low affinity ASE motifs appears to apply to some cases, it does not apply generally. The asymmetrically expressed *lsy-6* gene also contains a low-affinity ASE motif, as corroborated by competitive gel shift assays, but the two L/R asymmetrically expressed *gcy* genes *gcy-7* and *gcy-20* do not (Fig. 5D). Moreover, swapping the ASE motifs of the L/R asymmetric *gcy-7* and *gcy-22* genes with that of the bilateral, high-affinity *ceh-36* ASE motif does not cause de-repression in the contralateral neuron (data not shown). These findings further underscore the diversity of the cis-regulatory mechanisms that control L/R asymmetric gene expression.

An unusual class of *che-1* alleles separates the role of *che-1* in bilateral fate specification versus asymmetric subtype specification

Further insights into the importance of CHE-1 DNA-binding affinity with regard to the cis-regulatory logic of left/right asymmetric subtype specification were obtained by the recovery of an unusual class of *che-1* alleles. In a previously described screen for mutants that affect ASE specification, we described a mutant locus, *lsy-14*, that resulted in the conversion of ASEL fate to ASER fate, exemplified by ectopic expression of the ASER fate marker *gcy-5* in ASEL and a concomitant loss of the ASEL fate marker *lim-6* (Sarin et al., 2007) (Fig. 6A). This mutant phenotype is a characteristic phenotype of gene regulatory factors that act within the gene regulatory loop described in Fig. 1A. For example, *lsy-6* miRNA mutants cause a similar '2 ASER' phenotype as *lsy-14* mutants (Johnston and Hobert, 2003).

We mapped the *lsy-14(ot101)* locus to a small interval on chromosome I and obtained rescue of the mutant phenotype with a single fosmid (Table 1), which contains several genes, including *che-1*. A genomic fragment containing only the *che-1* locus also rescues *ot101* (Table 1). Moreover, *ot101* fails to complement the *che-1* null allele *ot66* (Table 1). We sequenced the *che-1* locus in *ot101* mutants and found a mutation in the linker region between zinc finger 1 and 2 (Fig. 6B). The identification of *ot101* as a *che-1* allele is an unexpected result as *che-1* null alleles cause a 'no ASEL/R' phenotype (class III phenotype), rather than a '2 ASER' (class II) phenotype (Chang et al., 2003). We then revisited some previously described *che-1* alleles, all of which had previously only been analyzed by expression of the *lim-6* ASEL fate marker, which is lost in all available *che-1* alleles (Sarin et al., 2007). We find that in three additional *che-1* alleles, the loss of *lim-6::gfp* is not a reflection of overall ASE fate loss as previously assumed, but is rather accompanied by de-repression of ASER fate (Table 1). All *che-1* alleles that cause the '2 ASER'/class II phenotype cluster around the second zinc finger (Fig. 6B).

Further investigating the class II phenotype of these *che-1* alleles, we find that the expression of four out of four tested bilaterally expressed markers is unaffected in *ot101* animals (Fig. 6A). Analyzing more asymmetric fate markers, we find that besides *gcy-5*, another ASER fate marker, *gcy-22* is de-repressed in ASEL and another ASEL fate marker besides *lim-6*, *gcy-7*, is lost, even though at much lower penetrance than the *lim-6* ASEL fate marker (Fig. 6A). The ASEL-restricted bistable loop component *lsy-6* is also affected, but the ASEL terminal fate marker *flp-4* is not (Fig. 6A). The distinct effect on different asymmetric markers suggests that *che-1(ot101)* does not simply affect a single regulatory component but may act independently on several different, ASE-motif containing, asymmetrically expressed genes. Consistent with this notion, *che-1(ot101)* displays complex interactions with components of the bistable feedback loop. The '2 ASEL' phenotype observed upon forced bilateral expression of the *lsy-6* miRNA is mildly affected by *ot101* in ASEL, and strongly affected in ASER (see Table S1 in the supplementary material). Forced bilateral expression of ASEL-fate inducer *die-1* is also affected by *ot101* in ASER, but not in ASEL (see Table S1 in the supplementary material). Taken together, class II *che-1* alleles have the unusual feature of not affecting bilateral fate specification of ASE, but modify the left/right subtype diversification program. The end result is a partial switch of ASEL to ASER fate. What are the molecular features of class II *che-1* alleles that might explain this effect?

Class II *che-1* alleles result in reduced DNA binding affinity

To understand the phenotype of class II *che-1* alleles in more detail, we examined the effect of these mutations on protein function. Notably, in contrast to strong loss of function or null alleles, which are either early nonsense mutations or reside in zinc finger 3 and 4 (Sarin et al., 2007), all class II alleles relate somehow to the second zinc finger of CHE-1. In *ot124*, *ot153* and *ot223*, the structural features of the second zinc finger are affected, including a residue that is directly involved in DNA binding (Fig. 6B). In *ot101*, the linker between the first and second zinc fingers is affected (Fig. 6B). Linker regions have previously been shown to be essential for DNA

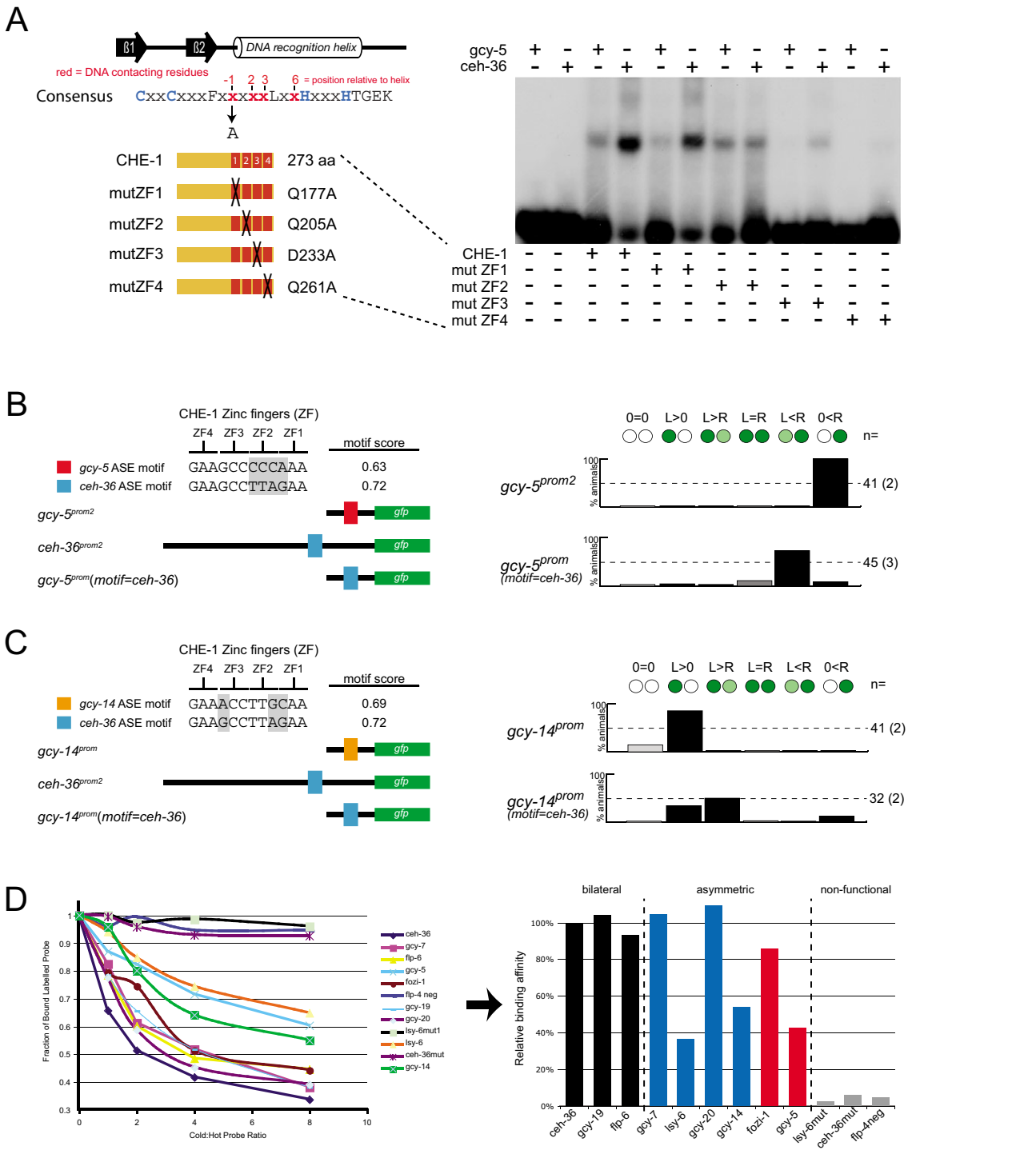

Fig. 5. Altering ASE motifs can disrupt L/R symmetric gene expression. (**A**) CHE-1 binds with higher affinity to the ASE motif of the *ceh-36* promoter versus that of the *gcy-5* promoter. The schematic on the left indicates the structure and consensus sequence of each C2H2 zinc finger with its DNA-contacting residues indicated in red. DNA contacts were abolished by mutating one of the DNA contacting residues in each zinc finger to an alanine. The right panel shows that wild-type CHE-1 shifts less *gcy-5* versus *ceh-36* probe. DNA binding of mutated CHA-1 protein (mutated as shown in left panel) demonstrates that three zinc fingers (2, 3 and 4) impact on CHE-1 binding to the ASE motif of *ceh-36*, whereas only two zinc fingers (3 and 4) impact on CHE-1 binding to the ASE motif of *gcy-5*. See Fig. S2 in the supplementary material for competitive gel shift that further solidifies the differential motif affinity. (**B**,**C**) Swapping the high-affinity ASE motif from the *ceh-36* promoter into the low-affinity motifs from *gcy-5* (B) or *gcy-14* (C) results in de-repression of *gfp* expression in the contralateral neuron. Multiple independent transgenic lines were scored (numbers shown in parentheses) and a representative line is shown. (**D**) Relative binding affinities of CHE-1 for various ASE motifs. The left panel shows results of quantitative EMSAs where binding to the ASE motif of a labeled *ceh-36* probe was competed with unlabeled ASE motifs from the genes indicated [sequences are the same as used by Etchberger et al. (Etchberger et al., 2007)]. In the right panel, the data are transformed into a graphical representation of binding affinities relative to the *ceh-36* probe (see Materials and methods). The lsy-mut probe mimics the *lsy-6(ot150)* mutation in ASE motif (Sarin et al., 2007). ceh-36mut abolishes expression of *ceh-36*^{prom}*::gfp* in vivo (data not shown).

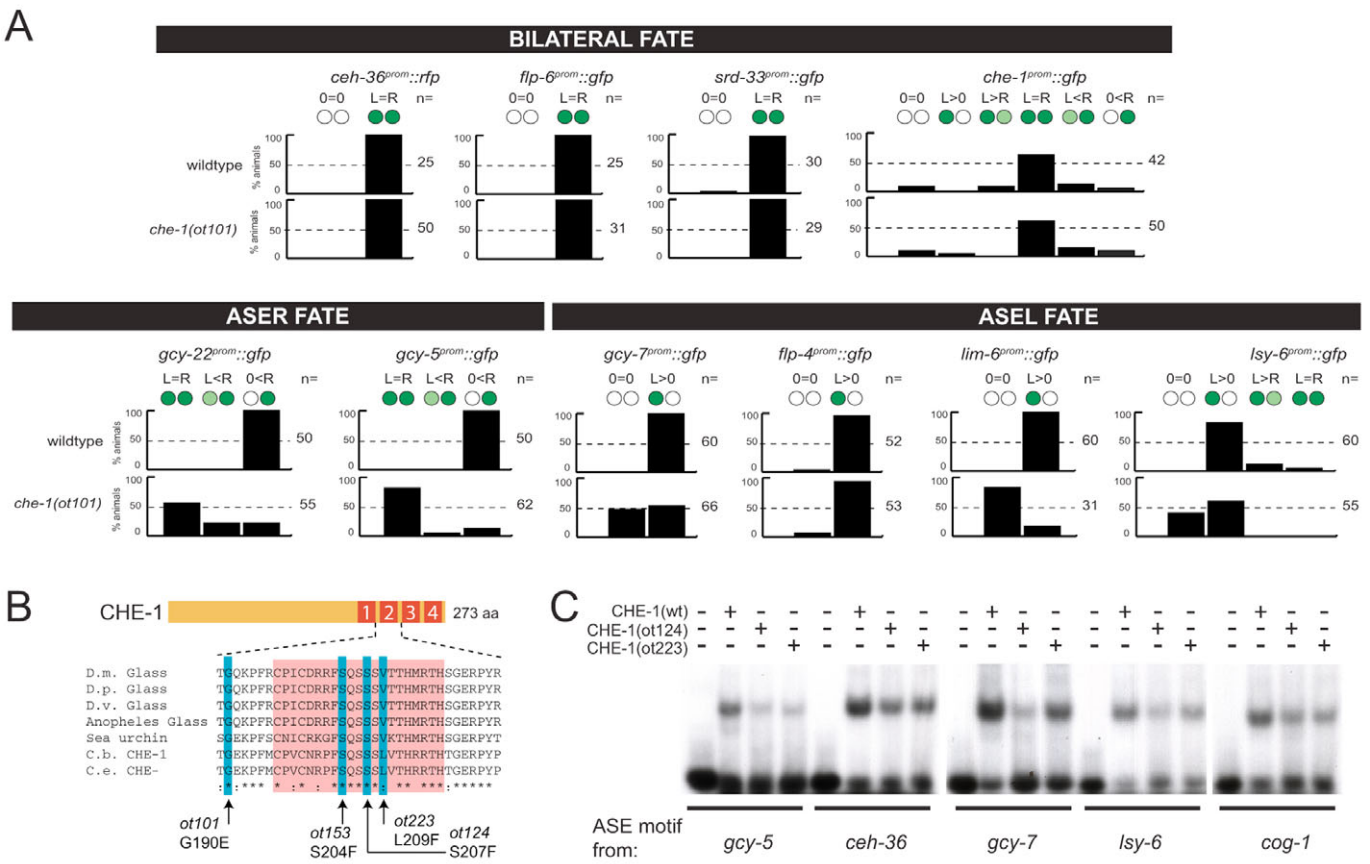

Fig. 6. Characterization of *che-1(ot101)*. (**A**) L/R asymmetric, but not bilateral ASE fate is affected in *che-1(ot101)* mutants. See Materials and methods for transgenes used. Pairs of green circles indicate ASE neuron pairs and relative *gfp* expression levels. (**B**) Molecular identity of class II *che-1* alleles. Alignment of the zinc fingers of *che-1* orthologs in other species (flies and sea urchin). The glycine in the linker position that is mutated in *ot101* is conserved in other linker regions within the Glass family, but also in many other zinc-finger proteins, including TFIIIA, Krueppel and others (data not shown). Note that zinc finger 3 and 4 touch the invariant part of part of the ASE motif and are absolutely crucial for DNA binding (Fig. 5) (Etchberger et al., 2007), whereas the class II alleles that affect zinc finger 2, which contact the less well conserved parts of the ASE motif, modulate only DNA binding, as shown in C. (**C**) Class II *che-1* alleles display reduced DNA-binding affinity. A representative gel shift experiment is shown.

binding of adjacent zinc fingers (Choo and Klug, 1993). We bacterially produced CHE-1 proteins that harbor the *ot124* and *ot223* point mutations in the second zinc finger. We find that each protein displays a decreased DNA-binding affinity across five different tested ASE motifs, both of high and low affinity (Fig. 6C). Even though it is unclear how mutations in zinc finger 2 interfere with overall DNA binding of CHE-1, we conclude that a reduction in DNA-binding activity causes a disruption of L/R asymmetrically expressed genes (hence, causing a class II *Lsy* phenotype), but leaving bilaterally expressed cis-regulatory control regions unaffected. This underscores the importance of DNA-binding affinity for controlling L/R asymmetric gene expression programs in the ASE neurons.

Raising *che-1* levels also disrupts cis-regulatory control of L/R asymmetrically expressed genes

Last, we also approached the *che-1*-binding site affinity issue from the angle of increasing ASE motif occupancy by raising the levels of wild-type CHE-1 protein. This may overcome the effect of co-repressor sites in asymmetrically expressed promoters and/or alleviate the need for a co-activator and thereby result in an ectopic expression of asymmetrically expressed genes in the contralateral neuron. We generated multicopy arrays of the *che-1* locus by injecting a fosmid containing the entire *che-1* locus into a wild-type background and then examined expression of two L/R asymmetrically expressed cis-regulatory regions (from the *gcy-5* and *gcy-7* locus). We find that both reporters become ectopically expressed in the contralateral neuron [29% of animals express *gcy-7* ectopically in ASER (n=65); 18% express *gcy-5* ectopically in ASEL (n=56); no contralateral expression of either gene is observed in wild-type animals]. It is not clear whether this effect is direct or mediated by intermediary regulatory components. This is the same issue as with the interpretation of the results of lowering of *che-1* activity in class II mutant alleles, in which we cannot definitely determine whether observed effects are direct or indirect. Nevertheless, we can conclude that increases or decreases in CHE-1 activity impact the left/right asymmetric execution of cell fate, while not affecting the ASE bilateral fate.

DISCUSSION

We can draw the following conclusions from our studies: (1) CHE-1 is not only required to induce ASE fate embryonically, but is also continuously required throughout the life of the neuron to maintain L/R asymmetric ASE cell fate; (2) in contrast to bilaterally expressed target genes of CHE-1, the regulation of asymmetrically expressed target genes involves the modulation of the activity of bilaterally expressed CHE-1 at the cis-regulatory level by additional

regulatory motifs which restrict CHE-1 activity in a target gene-dependent manner to either ASEL or ASER; (3) the binding affinity of CHE-1 to its target site plays an important role in restricting the CHE-1 activity to ASEL or ASER; (4) the cis-regulatory architecture that restricts CHE-1 activity in a L/R asymmetric manner is remarkably diverse. Rather than using a simple cis-regulatory motif (as is the case for ASE-motif/*che-1*-dependent ASEL/R bilateral specification), different L/R asymmetrically expressed genes appear to use distinct cis-regulatory strategies. We discuss those points and their implications individually below.

Maintenance of neuronal fate

The amenability of *C. elegans* to RNAi and the possibility to time its delivery allowed us to ask the fundamental question whether gene regulatory factors that turn on a specific terminal neuronal fate also are continuously required to maintain this fate throughout the life of the neuron. We find this to indeed be the case for the *che-1* transcription factor. Using a temperature-sensitive allele, such sustained function could also be demonstrated for the *unc-4* homeobox gene, which acts to determine specific synaptic inputs (Miller et al., 1992), but to our knowledge this issue has not been addressed for other regulatory factors that control neuronal differentiation in any system. Consistent with a maintenance function, *che-1* is expressed in the ASE neurons throughout the life of the animal (data not shown). Sustained *che-1* activity is ensured by *che-1* autoregulating its own expression via an ASE motif (Etchberger et al., 2007).

The continuous expression and requirement for *che-1* suggests that CHE-1 does not only have a role in initiating the terminal fate of ASE neurons, which is, immediately after the birth of the ASE neurons, initially bilaterally symmetric (Johnston et al., 2005). Rather, *che-1* also appears to be required for the progression of the hybrid precursor state to the L/R asymmetric terminal state. We infer this not only from the continuous expression and requirement of *che-1*, but also from the presence of functionally required ASE motifs in the cis-regulatory regions of L/R asymmetrically expressed genes. We can exclude the possibility that CHE-1 acts first to initiate L/R asymmetric genes via the ASE motif, and then to only indirectly restrict expression of L/R asymmetric genes in either ASEL or ASER, via the activation of intermediary transcription factors. If this were the case, our promoter analysis would have identified cis-regulatory motifs that can instruct ASE expression independently of the ASE motif. Even though we have found motifs that are required for activation of L/R asymmetric genes, these motifs only act in conjunction with the ASE motif. Moreover, the elimination of repressor motifs 'bilateralizes' the expression of normally L/R asymmetric genes, again arguing that bilateral CHE-1 is continually able to drive gene expression in both ASEL and ASER, but is prevented from doing so in a target gene-dependent manner.

Restriction of CHE-1 activity drives neuron subtype diversification

CHE-1 acts as a terminal selector gene that determines overall ASE fate by directly activating the expression of a large battery of bilaterally expressed genes (Etchberger et al., 2007; Hobert, 2008). In addition to this neuron class specification function of CHE-1, we have uncovered several cis-regulatory mechanisms that restrict CHE-1 activity on several target gene promoters to either the left or right ASE neuron, thereby driving a subtype specification program that diversifies these two cellular subtypes from one another (Fig. 7). The cis-regulatory mechanisms that restrict CHE-1 activity are promoter dependent and remarkably diverse. In three promoters (*lim-6*, *gcy-7*, *lsy-6*), we have found evidence for the existence of three distinct unrelated activator elements with which CHE-1 cooperates to promote L/R asymmetric expression. Notably, these activator elements are only required in the context of the complete regulatory module, as the ASE motif alone can drive bilateral ASE expression when in complete isolation, but is apparently not able to do so if in the context of the whole regulatory element. In such context, a cooperating activator motif is required for ASE expression (K50 binding site in *gcy-7* and bHLH binding site in *lsy-6*). It is possible that bilaterally expressed ASE motifs also require such positively cooperating factors.

Regulation of the *gcy-7* and *lsy-6* promoters, even though relying on distinct motifs, appears to share a similar logic. CHE-1 appears to be engaged in a tug-of-war with repressor elements in the promoter, which it can only overcome by the presence of an additional activator motif that cooperates with the ASE motif. The activator motif is only required if the repressor elements are present. If both are removed, CHE-1 exerts bilateral control over the promoter in both ASEL and ASER.

By contrast, no discrete repressor motifs were found in *lim-6* and no discrete co-activator motifs were found in *gcy-5*. It appears striking that none of the four promoters analyzed here uses similar strategies, as neither of the identified activator or repressor motifs show any similarity to one another. Moreover, even though some repressor motifs found to be required in one promoter (*gcy-7*) are present in other promoters (*gcy-14*, *gcy-20*), these motifs are not required in these other cases (data not shown). These findings may indicate an independent evolutionary recruitment of the many L/R asymmetrically expressed *gcy* genes into the regulatory network that controls L/R asymmetry of these neurons. This diversity is consistent with differences in the expression of *gcy* genes in different nematode species (Ortiz et al., 2006). This plasticity in the composition of the L/R asymmetric terminal features may relate to the sensory function of ASE neurons that may need to adapt to distinct environmental cues in a species-specific manner.

Previous genetic analysis has revealed several candidates for activator and repressor factors that may act through the cis-regulatory elements that we have described here to restrict CHE-1 activity (Fig. 1A). These include the zinc-finger transcription factor DIE-1 [genetically required to activate ASEL-expressed genes and repress ASER-expressed genes (Chang et al., 2004)], the LIM homeodomain protein LIM-6 [required to repress *gcy-5* in ASEL (Hobert et al., 1999), Fig. 1A], the zinc-finger protein FOZI-1 [required to repress *gcy-7* in ASER (Johnston et al., 2006), Fig. 1A], and two other, as yet uncloned *lsy* genes with similar phenotypes to *lim-6* [*lsy-20* and *lsy-26* (Sarin et al., 2007)]. DNA-binding sites are not known for DIE-1, LIM-6 or FOZI-1, and in vitro gelshift assays have not detected binding of these factors to ASEL or ASER-specific promoters (data not shown). However, the putative K50-homeodomain binding site identified in the *gcy-7* promoter is a likely binding site for the CEH-36/Otx homeodomain protein. CEH-36 binds to the motif in vitro and *gcy-7* fails to be activated in *ceh-36* mutants. The asymmetric, ASEL-fate inducing activity of CEH-36 is also evident at the cis-regulatory level as the CEH-36 binding site will convert a bilaterally expressed ASE motif into a regulatory motif that is more strongly expressed in ASEL than in ASER (ASE-gcy-7#2 construct in Fig. 4). Therefore, CEH-36 activity must be somehow lateralized, even though CEH-36 is expressed in both ASEL and ASER.

Another factor that contributes to the restriction of CHE-1 activity is the affinity of the CHE-1/ASE motif interaction, which we again find to be important for some, but not all, promoters. The affinity

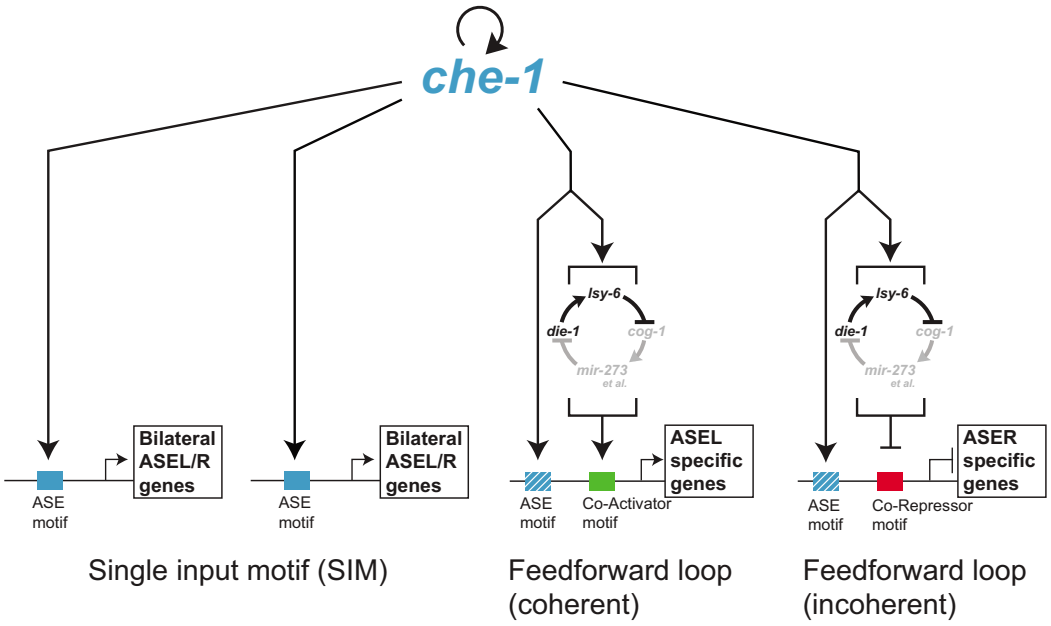

Fig. 7. CHE-1 acts in the context of many gene regulatory network motifs. CHE-1 autoregulates its own expression via an ASE motif (Etchberger et al., 2007) and co-regulates many bilaterally expressed target genes by what has been termed a 'single input motif' (Alon, 2007). Further diversification programs downstream of CHE-1, which result in differential gene expression in ASEL versus ASER, involve a more complex version of a feed-forward loop (FFL) motif (see text). Depending on the signs of the regulatory interactions, these motifs can be coherent or incoherent (Alon, 2007). The bracket indicates that CHE-1 directly regulates the expression of multiple bistable feedback loop components (Fig. 1A) via ASE motifs. Multiple additional network motifs are also embedded here, as discussed previously (Hobert, 2006). For example, *die-1* affects *gcy-7* expression via *fozi-1* in what appears to be an embedded FFL (Johnston et al., 2006). Note that the ASE motif in the asymmetrically expressed genes is stippled to indicate that, at least in some cases, intrinsic features of the ASE motif (i.e. its affinity to ASE) play a role in determining the laterality of gene expression. The model shown here applies to the ASEL neuron (ASEL genes activated; ASER genes repressed); the opposite holds for the ASER neuron.

argument stems largely from three observations. First, swapping a high-affinity ASE motif from a bilateral promoter into that of two different asymmetric promoters results in the partial bilateralization of promoter activity. We interpret this to mean that, at least in some cases, CHE-1 binding to the ASE motif is weak so as to make it susceptible to the effect of repressor motifs. Increases in the affinity of the CHE-1-binding site counteract the repressive effect. Second, increases in CHE-1 expression disrupt L/R asymmetric promoter activity. Third, we have identified an unusual class of alleles of *che-1*, which separates the activity of *che-1* on bilaterally expressed versus L/R asymmetrically expressed promoters. These alleles cause a general decrease in ASE motif affinity and lead to a disruption of L/R asymmetric gene expression, while leaving bilateral expression intact. We note, however, that the importance of affinity may not be a general theme as not all motif swaps yielded the same results and the effect of the unusual *che-1* alleles does not extend to every single L/R asymmetrically expressed gene.

Although CHE-1 activity must somehow be integrated with other transcription factors such as CEH-36, which are genetically required for L/R asymmetry, we also note another, as yet completely unexplored, layer of regulatory control that may play a role in the system. All cis-regulatory elements described here (including the ASE motifs) are located in remarkable vicinity to predicted translational start sites and hence may be components of the RNA-Pol II-binding core promoter. Unfortunately, owing to the phenomenon of trans-splicing, transcriptional start sites and

Table 1. Phenotypic analysis of *che-1* alleles

Genotype	ASEL fate marker (lim-6)	ASER fate marker (gcy-5)	ASEL/R (ceh-36)	Mutant class
Wild type	0% (*n*>100) lost	0% (*n*>100) ectopic in ASEL	0% (*n*>100) lost	–
*ot101**	83% (*n*=31) lost	72% (*n*=60) ectopic in ASEL	0% (*n*=50) lost	Class II
ot101; Ex[che-1]†	0% (*n*=50) lost	23% (*n*=65) ectopic in ASEL	n.a.	Class II
ot66‡	100% (*n*=50) lost	100% (*n*=50) lost	100% (*n*=50) lost	Class III
ot101/ot66	n.d.	96% (*n*=69) ectopic in ASEL	n.a.	Class II
ot124	100% (*n*=50) lost	78% (*n*=58) ectopic in ASEL	0% (*n*=50) lost	Class II
ot153	100% (*n*=50) lost	80% (*n*=50) ectopic in ASEL	45% (*n*=35) lost	Class II
ot223	100% (*n*=50) lost	67% (*n*=51) ectopic in ASEL	78% (*n*=50) lost	Class II

%, fraction of animals in population with given phenotype. The data for the ASEL fate marker expression in *ot124, ot153* and *ot223* have been previously reported (Sarin et al., 2007), but ASER fate has not previously been examined. Fate marker are *otIs114 (lim-6::gfp)*, *ntIs1 (gcy-5:gfp)*, *otIs214 (gcy-5mChopti)* and *otIs151 (ceh-36::rfp).*
*These data are also shown graphically in Fig. 6 and in Sarin et al. (Sarin et al., 2007), and are shown here for comparison only.
†The ASEL defect was rescued with the *che-1* locus contained within the fosmid WRM0634dB09 and the ASER defect with a PCR amplicon of the *che-1* locus from the gene 5′ of *che-1* up to and including the 3′ UTR of *che-1*. In each case, three lines were tested, three rescued and one line is shown.
‡Putative null allele from Chang et al. (Chang et al., 2003).

hence core promoter sites are difficult to map in *C. elegans*. As previous work in other systems has shown shifts in core promoter selectivity during development (Juven-Gershon et al., 2008), it will be intriguing to investigate how the regulatory elements defined here relate to Pol II function.

Feed-forward loops may be a general component of cellular subtype specification programs

The findings described here provide insights into how cellular fates become progressively restricted during development. Transcriptional regulators often define broad domains of gene expression that become further restricted, refined and diversified through added layers of regulatory control. In the context of terminal neuronal differentiation, an important class of regulatory proteins are what we term 'terminal selector genes' (Hobert, 2008). These encode for transcription factors that determine the terminal identity of individual neuron types by directly controlling the expression of terminal gene batteries. CHE-1 is such a terminal selector gene, which directly controls the expression of a large battery of cell fate markers that are shared by ASEL and ASER (Etchberger et al., 2007). Other examples for terminal selector genes can not only be found in *C. elegans* but also in vertebrates, particularly in the brain (Hobert, 2008). Although terminal selector genes define the properties of individual neuron classes, ensuing subtype specification events further diversify neuron classes, as is the case in the diversification of the ASEL and ASER subtypes.

Together with our previous analysis of gene regulatory factors in ASE, the data presented here demonstrates that terminal selector genes participate directly in the subtype diversification that follows neuron type specification. The way that CHE-1 achieves this feat may reveal a common theme in gene regulatory networks that serve to diversify gene expression programs. CHE-1 interacts with other regulatory modules in a feed-forward loop (FFL) motif configuration. A conventional FFL consists of a transcription factor A, controlling factor B, and factor A and B controlling together a target C (Alon, 2007). Such simple FFL motifs can have specific properties such as persistence detection or response acceleration. CHE-1 acts in a more complicated version of the FFL. Besides activating a single transcription factor (CEH-36) with which it collaborates to regulate the expression of a target gene (*gcy-7*), CHE-1 also activates multiple components of the bistable regulatory loop shown in Fig. 1A; the regulatory loop provides a net activity output that then cooperates with CHE-1 in a promoter-specific manner on a given target gene (Fig. 7). For some genes, the loop provides a positive output with which CHE-1 needs to interact to be able to turn on a target gene (e.g. *lim-6* in ASEL). For other target genes, the loop provides a negative output (e.g. in the form of the LIM-6) that restricts the ability of CHE-1 to turn on a target gene (e.g. prevents the activation of *gcy-5* in ASEL).

Apart from whatever precise kinetic properties such network motif configuration may convey, one may view such network architecture as being reflective of the evolution of gene regulatory networks. The two ASE neurons may have initially been identical, with CHE-1 controlling the exact same set of genes in ASEL and ASER. This ancestral state may still be reflected ontogenetically in the hybrid precursor state through which CHE-1 passes after the ASE neurons are born. As a segregation of certain features (such as chemoreceptors) into distinct cells (i.e. ASEL and ASER) can convey beneficiary selective advantages to an animal [increases in discriminatory properties (Pierce-Shimomura et al., 2001; Suzuki et al., 2008)], additional regulatory mechanisms may have been implemented downstream of CHE-1 to restrict CHE-1 activity to a subset of target genes (Fig. 7).

Even though not dissected to the same extent as the ASE system, FFL-loop dependent subtype specification mechanisms also occur in other systems, such as the vertebrate retina (Hsiau et al., 2007) or in the fly ventral nerve cord (Baumgardt et al., 2007), and may provide a commonly used regulatory logic for subtype specification.

We thank B. Tursun (Columbia University) for providing *otIs188* and for communicating unpublished results, N. Flames for the control shown in Fig. 3A, Q. Chen for expert DNA injection and members of the Hobert laboratory for comments on the manuscript. We acknowledge funding by the NIH (R01NS039996-05; R01NS050266-03). O.H. is an Investigator of the HHMI. Deposited in PMC for release after 6 months.

Supplementary material

Supplementary material for this article is available at http://dev.biologists.org/cgi/content/full/136/1/147/DC1

References

Ahringer, J. (2005). Reverse genetics. In *WormBook* (ed. The C. elegans Research Community). WormBook: www.wormbook.org.

Alon, U. (2007). Network motifs: theory and experimental approaches. *Nat. Rev. Genet.* **8**, 450-461.

Baumgardt, M., Miguel-Aliaga, I., Karlsson, D., Ekman, H. and Thor, S. (2007). Specification of neuronal identities by feedforward combinatorial coding. *PLoS Biol.* **5**, e37.

Cartharius, K., Frech, K., Grote, K., Klocke, B., Haltmeier, M., Klingenhoff, A., Frisch, M., Bayerlein, M. and Werner, T. (2005). MatInspector and beyond: promoter analysis based on transcription factor binding sites. *Bioinformatics* **21**, 2933-2942.

Chang, S., Johnston, R. J., Jr and Hobert, O. (2003). A transcriptional regulatory cascade that controls left/right asymmetry in chemosensory neurons of C. elegans. *Genes Dev.* **17**, 2123-2137.

Chang, S., Johnston, R. J., Frokjaer-Jensen, C., Lockery, S. and Hobert, O. (2004). MicroRNAs act sequentially and asymmetrically to control chemosensory laterality in the nematode. *Nature* **430**, 785-789.

Choo, Y. and Klug, A. (1993). A role in DNA binding for the linker sequences of the first three zinc fingers of TFIIIA. *Nucleic Acids Res.* **21**, 3341-3346.

Etchberger, J. F., Lorch, A., Sleumer, M. C., Zapf, R., Jones, S. J., Marra, M. A., Holt, R. A., Moerman, D. G. and Hobert, O. (2007). The molecular signature and cis-regulatory architecture of a C. elegans gustatory neuron. *Genes Dev.* **21**, 1653-1674.

Glass, C. K., Holloway, J. M., Devary, O. V. and Rosenfeld, M. G. (1988). The thyroid hormone receptor binds with opposite transcriptional effects to a common sequence motif in thyroid hormone and estrogen response elements. *Cell* **54**, 313-323.

Hobert, O. (2002). PCR fusion-based approach to create reporter gene constructs for expression analysis in transgenic C. elegans. *Biotechniques* **32**, 728-730.

Hobert, O. (2006). Architecture of a MicroRNA-controlled gene regulatory network that diversifies neuronal cell fates. *Cold Spring Harb. Symp. Quant. Biol.* **71**, 181-188.

Hobert, O. (2008). Regulatory logic of neuronal diversity: terminal selector genes and selector motifs. *Proc. Natl. Acad. Sci. USA* (in press).

Hobert, O., Tessmar, K. and Ruvkun, G. (1999). The Caenorhabditis elegans lim-6 LIM homeobox gene regulates neurite outgrowth and function of particular GABAergic neurons. *Development* **126**, 1547-1562.

Hobert, O., Johnston, R. J., Jr and Chang, S. (2002). Left-right asymmetry in the nervous system: the Caenorhabditis elegans model. *Nat. Rev. Neurosci.* **3**, 629-640.

Hsiau, T. H., Diaconu, C., Myers, C. A., Lee, J., Cepko, C. L. and Corbo, J. C. (2007). The cis-regulatory logic of the mammalian photoreceptor transcriptional network. *PLoS ONE* **2**, e643.

Johnston, R. J. and Hobert, O. (2003). A microRNA controlling left/right neuronal asymmetry in Caenorhabditis elegans. *Nature* **426**, 845-849.

Johnston, R. J., Jr, Chang, S., Etchberger, J. F., Ortiz, C. O. and Hobert, O. (2005). MicroRNAs acting in a double-negative feedback loop to control a neuronal cell fate decision. *Proc. Natl. Acad. Sci. USA* **102**, 12449-12454.

Johnston, R. J., Jr, Copeland, J. W., Fasnacht, M., Etchberger, J. F., Liu, J., Honig, B. and Hobert, O. (2006). An unusual Zn-finger/FH2 domain protein controls a left/right asymmetric neuronal fate decision in C. elegans. *Development* **133**, 3317-3328.

Juven-Gershon, T., Hsu, J. Y., Theisen, J. W. and Kadonaga, J. T. (2008). The RNA polymerase II core promoter-the gateway to transcription. *Curr. Opin. Cell Biol.* **20**, 253-259.

Lanjuin, A., VanHoven, M. K., Bargmann, C. I., Thompson, J. K. and Sengupta, P. (2003). Otx/otd homeobox genes specify distinct sensory neuron identities in C. elegans. *Dev. Cell* **5**, 621-633.
Masland, R. H. (2004). Neuronal cell types. *Curr. Biol.* **14**, R497-R500.
Miller, D. M., Shen, M. M., Shamu, C. E., Burglin, T. R., Ruvkun, G., Dubois, M. L., Ghee, M. and Wilson, L. (1992). C. elegans unc-4 gene encodes a homeodomain protein that determines the pattern of synaptic input to specific motor neurons. *Nature* **355**, 841-845.
Nelson, S. B., Hempel, C. and Sugino, K. (2006). Probing the transcriptome of neuronal cell types. *Curr. Opin. Neurobiol.* **16**, 571-576.
Noyes, M. B., Christensen, R. G., Wakabayashi, A., Stormo, G. D., Brodsky, M. H. and Wolfe, S. A. (2008). Analysis of homeodomain specificities allows the family-wide prediction of preferred recognition sites. *Cell* **133**, 1277-1289.
Ortiz, C. O., Etchberger, J. F., Posy, S. L., Frokjaer-Jensen, C., Lockery, S., Honig, B. and Hobert, O. (2006). Searching for neuronal left/right asymmetry: genomewide analysis of nematode receptor-type guanylyl cyclases. *Genetics* **173**, 131-149.
Pierce-Shimomura, J. T., Faumont, S., Gaston, M. R., Pearson, B. J. and Lockery, S. R. (2001). The homeobox gene lim-6 is required for distinct chemosensory representations in C. elegans. *Nature* **410**, 694-698.
Ramon y Cajal, S. (1911). *Histologie du système nerveux de l'homme et des vertébrés*. Paris: Maloine.
Sarin, S., O'Meara, M. M., Flowers, E. B., Antonio, C., Poole, R. J., Didiano, D., Johnston, R. J., Jr, Chang, S., Narula, S. and Hobert, O. (2007). Genetic screens for caenorhabditis elegans mutants defective in left/right asymmetric neuronal fate specification. *Genetics* **176**, 2109-2130.
Schmitz, C., Kinge, P. and Hutter, H. (2007). Axon guidance genes identified in a large-scale RNAi screen using the RNAi-hypersensitive Caenorhabditis elegans strain nre-1(hd20) lin-15b(hd126). *Proc. Natl. Acad. Sci. USA* **104**, 834-839.
Sulston, J. E., Schierenberg, E., White, J. G. and Thomson, J. N. (1983). The embryonic cell lineage of the nematode Caenorhabditis elegans. *Dev. Biol.* **100**, 64-119.
Suzuki, H., Thiele, T. R., Faumont, S., Ezcurra, M., Lockery, S. R. and Schafer, W. R. (2008). Functional asymmetry in Caenorhabditis elegans taste neurons and its computational role in chemotaxis. *Nature* **454**, 114-117.
Treisman, J., Gonczy, P., Vashishtha, M., Harris, E. and Desplan, C. (1989). A single amino acid can determine the DNA binding specificity of homeodomain proteins. *Cell* **59**, 553-562.
Uchida, O., Nakano, H., Koga, M. and Ohshima, Y. (2003). The C. elegans che-1 gene encodes a zinc finger transcription factor required for specification of the ASE chemosensory neurons. *Development* **130**, 1215-1224.
Yu, S., Avery, L., Baude, E. and Garbers, D. L. (1997). Guanylyl cyclase expression in specific sensory neurons: a new family of chemosensory receptors. *Proc. Natl. Acad. Sci. USA* **94**, 3384-3387.